International Journal of Heat and Fluid Flow 30 (2009) 637–646

Contents lists available at ScienceDirect

International Journal of Heat and Fluid Flow

journal homepage: www.elsevier.com/locate/ijhff

Investigation of the specific mass flow rate distribution in pipes supplied with a pulsating flow

Aleksander Olczyk *

Institute of Turbomachinery, Technical University of Lodz, Wolczanska 219/223, 90-924 Lodz, Poland

ARTICLE INFO

Article history:
Received 11 August 2008
Received in revised form 6 February 2009
Accepted 14 February 2009
Available online 25 March 2009

Keywords:
Pulsating flow
Unsteady flow measurement
Calibration
Correction
Uncertainty
Profile

ABSTRACT

A pulsating flow is typical of inlet and exhaust pipes of internal combustion engines and piston compressors. Unsteady flow phenomena are especially important in the case of turbocharged engines, because dynamic effects occurring in the exhaust pipe can affect turbine operation conditions and performance.

One of the basic parameters describing the unsteady flow is a transient mass flow rate related to the instantaneous flow velocity, which is usually measured by means of hot-wire anemometers. For the flowing gas, it is more appropriate to analyze the specific mass flow rate $\varphi_m = \rho v$, which takes into account also variations in the gas density. In order to minimize the volume occupied by measuring devices in the control section, special double-wire sensors for the specific mass flow rate (CTA) and temperature (CCT) measurement were applied. The article describes procedures of their calibration and measurement. Different forms of calibration curves are analyzed as well in order to match the approximation function to calibration points. Special attention is paid to dynamic phenomena related to the resonance occurring in a pipe for characteristic frequencies depending on the pipe length. One of these phenomena is a reverse flow, which makes it difficult to interpret properly the recorded CTA signal. Procedures of signal correction are described in detail. To verify the measurements, a flow field investigation was carried out by displacing probes radially and determining the profiles of the specific mass flow rate under the conditions of a steady and pulsating flow. The presence and general features of a reverse flow, which was identified experimentally, were confirmed by 1-D unsteady flow calculations.

1. Introduction

A pulsating flow is usually found in inlet and exhaust pipes of internal combustion engines and piston compressors. Owing to the cyclic character of operation (the periodical opening and closing of valves), the flow of gases is unsteady and it becomes periodical for a fixed operation point. The pulse frequency f depends on the number of cylinders i_C and the rotational speed of the engine n [rev/min]:

$$f = k_s \cdot i_C \cdot \frac{n}{60} \tag{1}$$

The coefficient $k_s = 1$ for 2-stroke or $k_s = \frac{1}{2}$ for 4-stroke engines, as the intake or the exhaust takes place every second engine revolution. For a typical arrangement (a 4-stroke engine with 4 cylinders) of the diesel engine with the maximum rotational speed $n_{max} = 6000$ rev/min, we obtain $f_{max} = 200$ Hz and this value defines the range of frequencies to be examined in the study.

A flow of gases in pipes is usually described by three parameters, namely: pressure (p) temperature (T) and velocity (v), which is related to the volumetric ($\dot{V}$) or mass ($\dot{m}$) flow rate. In the case of a pulsating flow, these parameters become time-dependent functions and along with their spatial distribution $F_{(x,y,z)}$, their temporal variations $F_{(t)}$ should be investigated. Transient velocities $v_{(t)}$ can be measured by different methods, however only two of them have practical significance, i.e., laser optical techniques (LDA or PIV) and thermal anemometry (HWA). Optical techniques remain much more expensive and laborious than hot-wire anemometry, which is more available and ensures excellent dynamic properties and accuracy of the applied sensors (Witze, 1980).

In the case of inlet and exhaust pipes, 1-D models are traditionally applied due to their simplicity (Chalet et al., 2006). These models usually ensure a similar level of accuracy as advanced and laborious 3-D simulations, which require an assumption of the proper turbulence model (Kirkpatrick et al., 1994). For a 1-D flow description, only the axial velocity component $v = v_x$ is used and it must be representative of the entire control section under consideration. In the case of the HWA application, a single point measurement is executed and a question arises whether the obtained results can be used as parameters describing correctly the flow

* Tel.: +48 42 631 23 84; fax: +48 42 636 13 83.
E-mail address: aolczyk@p.lodz.pl

0142-727X/$ - see front matter © 2009 Elsevier Inc. All rights reserved.
doi:10.1016/j.ijheatfluidflow.2009.02.006

in the section analyzed. An application of 1-D models requires elementary knowledge of the velocity distribution in the investigated control sections of the pipe and it should be verified if the point measurement of the velocity/specific mass flow rate, which is usually made near the pipe axis, can be used for a correct and complete flow description in these sections. In the case of planar velocity fields, this verification can be conducted by means of PIV methods as described in Breuer et al. (2000) or by conducting the flow field survey through displacing the hot-wire probe as described in a further part of this paper.

It should be remarked that under the conditions of a pulsating flow, the dynamic phenomena occurring at certain conditions can considerably affect either transient or mean flow parameters. One of these effects is a reverse flow that may occur in the pipe near to the resonance (Olczyk 2007, in press). An identification of this effect is extremely important as the hot-wire anemometer cannot distinguish between a forward and reverse flow and measurement results can be erroneous if not corrected, which leads to improper calculation results consequently (Jau-Huai Lu, et al., 1998). More advanced methods of the reverse flow identification as the pulsed hot-wire technique PWA (Bruun, 1999; Handford and Bradshaw, 1989) or the flying hot-wire technique FWA (Bruun, 1999; Thompson and Whitelaw, 1984) can be also applied, however they require specially designed probes and accessories, which makes them more expensive and less available. An interesting method to investigate an interface between the forward and reverse flow region localization was presented in Sokolov and Ginat (1992), where the authors described a ladder-like probe consisting of a rake of 16 wires permitting to describe precisely the thickness of the reverse flow region. Procedures of the true (de-rectified) signal reconstruction were also presented. Their principle is generally the same as applied in a further part of the present paper.

The results of experiments which will be presented in a further part of the paper were obtained during the tests of a pulsating flow. Their aim was to verify correctness of the "*x*–*t*" model of the 1-D flow (Olczyk and Sobczak, 2008), validate an acoustic approach for resonance frequencies determination and study behavior of various piping systems under the conditions of a pulsating flow (Olczyk, in press). In the present paper, only the aspect of the specific mass flow rate measurement will be considered.

2. Test rig configuration

The test rig was designed to simulate dynamic flow phenomena which may occur in inlet or exhaust pipes under the conditions of a pulsating flow. The piping system composed of straight circular pipes of a diameter equal to ∅42 mm was supplied with warm, compressed air through the pulse generator (Fig. 1b) described in (Olczyk, 2007), providing a periodical variation of flow parameters in the range of frequencies f = 0–200 Hz. An idea of pulse generation consists in a cyclic deceleration of the flowing gas by a rotating element (a rotating valve). The pulse frequency is controlled by changing the rotational speed of the electric motor by means of a frequency inverter. Generally, the test rig was arranged for investigations of unsteady flow phenomena in pipes connected to an automotive turbocharger (Fig. 1a). Other combinations with different pipe discharge configurations were also investigated in order to enlarge the scope of research, namely: a pipe open at the end and a pipe with a large volume tank or with a nozzle at the end (see Olczyk (in press)).

In all cases, the common elements of the test stand were as follows (Fig. 1a):

- a system of air heating composed of a set of electric heaters AHF-14240 (Heat – Omega 2000), permitting to increase the temperature at the turbine inlet up to 100–120 °C;
- a pulse generator (Gen) with speed controlled by a frequency inverter;
- a tested pipe mounted between control sections (0) and (3). Two different lengths were used: L_S = 0.544 m (a short pipe) and L_L = 1.246 m (a long pipe);
- a set of valves (V_C,V_T) permitting to control the mass flow rate and the turbocharger operation point.

Measurements of transient and mean values of pressure, temperature and specific mass flow rate were conducted in control sections (0) and (3) (Fig. 1a). Additionally, transient pressure was measured in section (*K*) placed in the pipe mid length.

As far as measurement devices are concerned, the following equipment was used:

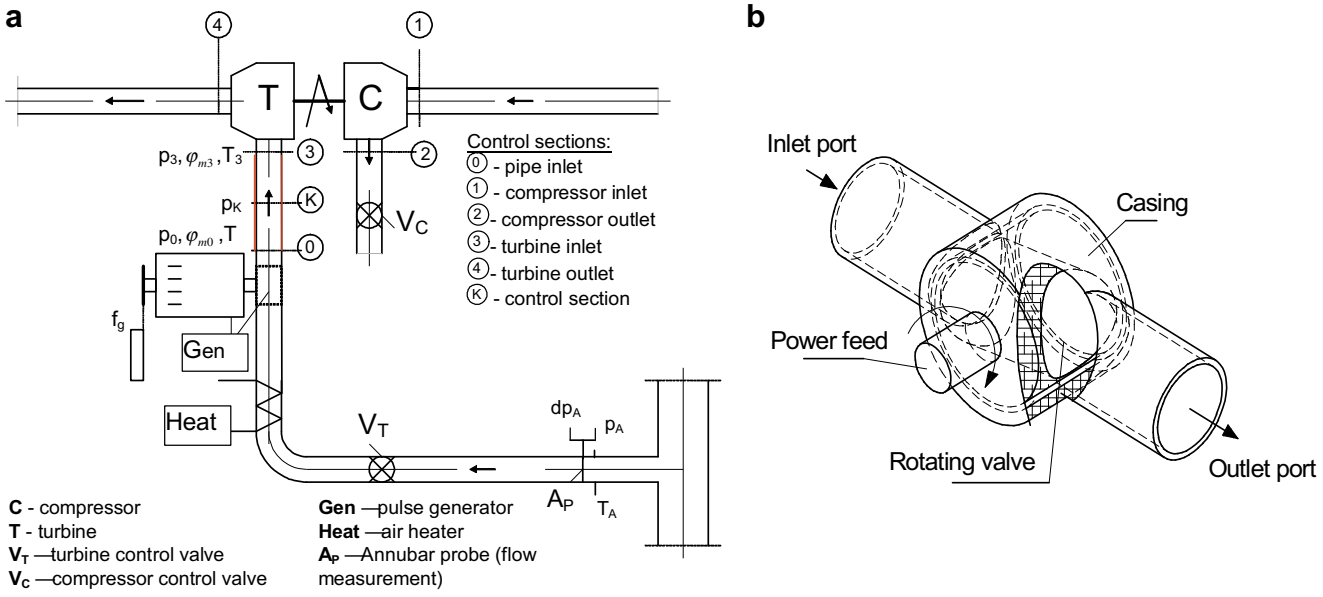

Fig. 1. Schemes of the test rig (a) and the pulse generator (b).

– piesoresistive transducers for pressure measurements: Endevco 8510C-15 and 8510C-50 (Endevco 2003);
– constant current thermometers (CCT) for temperature measurements (Olczyk, 2008a);
– constant temperature anemometers (CTA) for specific mass flow rate measurements.

Both CCT and CTA probes incorporated a 5 μm tungsten wire. According to Bruun (1999), the frequency limits for this wire diameter are: 1×10^2 Hz for a CCT and 1×10^5 Hz for CTA probe, respectively. Both thin-wire probes employed the same wire-holder (Olczyk, 2008a) to limit the space occupied by the sensor in the pipe. To avoid the reciprocal influence of the wires, a 3 mm offset was applied in their radial position.

Upstream of the pulse generator, a standard flowmeter – a multihole impact probe (an Annubar probe – Dieterich Standard, 1995) – was mounted. Its brief description will be presented in Section 3.

3. Calibration of the CTA

The CTA calibration curve is most often expressed as a relationship between the output voltage signal U and the flow velocity v. Its form is usually based on the classical King's equation (King, 1914):

$$U^2 = A + Bv^n \tag{2}$$

where A, B, n are the coefficients yielded by the approximation procedure.

Many attempts were made to ensure better matching of the approximating equation to the experimentally obtained calibration points. Two of them can be mentioned:

– the exponent n is expressed as a velocity function $n = n(v)$ (Elsner and Gudlach, 1973);
– the exponent n is assumed to be constant $n = 0,5$ and an additional correction term Cv (Shibl, 1987) is introduced:

$$U^2 = U_0^2 + Bv^{0.5} + Cv \tag{3}$$

The pulsating flow of the gas in exhaust pipes is characterized by high amplitudes of all main flow parameters. As a consequence, the flow density ρ should also be considered to be variable and included when the CTA output signal U is analyzed. Therefore, it is more adequate to use the specific mass flow rate φ_m defined as:

$$\varphi_m = \rho v = \frac{\dot{m}}{S} \tag{4}$$

where $\dot{m}$ denotes the mass flow rate traversing a control section of the area S. The output signal depends also on the difference between two unknown temperatures: of the wire T_w and of the gas T_g, therefore the following relationship (compare Eq. (2)) can be obtained (Cimbala and Park, 1990):

$$U^2 = A' + B'(\rho v)^N (T_w - T_g) \tag{5}$$

In the CTA mode, the wire temperature T_w is kept constant by the electronic control system, but the gas temperature T_g can vary. The problem of temperature variation during hot-wire measurements was analyzed in a large number of studies (Savostenko and Serbin, 1988; Sakao, 1973; Bremhorst and Graham, 1990) and various solutions to this problem were proposed to ensure a satisfactory bandwidth of transmitted signals (Ligęza, 2008). In the case presented here, the simplest solution was applied – the temperature of the flowing gas was kept constant during the calibration (in the presented tests, it was stabilized at approximately 40 °C, which corresponded to the mean value expected for further measurements under the conditions of a pulsating flow). Maintaining the temperature at a fixed level permits us to ignore the temperature influence on the hot-wire output signal (see Eq. (5)).

In practice, during measurements, the inverse characteristic curve $\dot{m} = f(U)$ or $\varphi_m = f(U)$ is more useful. The King's equation and the related relationships are inconvenient here, especially in the case of the variable n (as the approximation procedure has to be conducted iteratively). Therefore, another formula, proposed by TSI (TSI Inc.) and expressed by means of the 4th order polynomial, is often applied:

$$\varphi_m = A_0 + A_1 U + A_2 U^2 + A_3 U^3 + A_4 U^4 \tag{6}$$

where A_0, …, A_4 – coefficients determined in the calibration procedure.

An example calibration characteristic curve approximated by means of Eq. (6) is presented in Fig. 2a and, as can be seen, it describes a shape of the hot-wire characteristics quite well. However, in some cases its application can make the approximation ambiguous. This particular case is shown in Fig. 2b. In the range of low specific mass flow rates, approximating curve (1) is ambiguous (a kind of a "saddle" appears) and the characteristic curve cannot be used in this form. Usually this situation occurs when the range of calibration is not sufficiently wide (compare the U and φ_m ranges for Fig. 2a and b) and the number of points of calibration in the initial range of the characteristics is insufficient to describe it correctly.[1]

In such a case, an application of the exponential growth function can be considered:

$$\varphi_m = A_0 + A_1 e^{\left(\frac{U}{B}\right)} \tag{7}$$

This equation (curve (2) – Fig. 2b) is free of the ambiguity defect and yields the correct approximation in the range of low mass flow rates. At higher mass flow rates, the plot is in fact equivalent to the 4th order polynomial (compare curves (1) and (2) – Fig. 2b). However, for high mass flow rates, the exponential curve becomes steeper than the polynomial, which overestimates the mass flow rate. Generally, the condition of similar mass flow rate ranges during calibration and measurement[2] should be satisfied to avoid these ambiguities.

The calibration was conducted under steady flow conditions: the pulse generator (Fig. 1) remained in a fully open position. A multihole impact probe (Annubar probe – Dieterich, 1995) was applied as the standard flowmeter. It was mounted upstream of the pulse generator (Fig. 1a) in order to prevent it from the influence of pulsations. However, the calibration was carried out under the conditions of a steady flow but the Annubar probe was also used during measurements for the pulsating flow conditions for comparative purposes (see Section 4). Its position was chosen to avoid the backward action of the pulse generator. Heating elements (Fig. 1a) helped in damping potential backward pulsations.

The Annubar probe operates by sensing an impact pressure and a reference pressure through multiple sensing ports located on the upstream and downstream sides of the probe. The resultant pressure difference Δp_A is related to the mean mass flow rate $\dot{m}_{ref}$ averaged by the surface of the pipe cross-section.[3]

The mass flow rate $\dot{m}_{ref}$ measured by the Annubar probe can be expressed as (Dieterich, 1995):

[1] Usually it is difficult to ensure accurate measurement for low velocities during the hot-wire calibration and special calibration procedures should be applied (Bruun et al. 1989; Al-Garni, 2007).

[2] It should be noted that the calibration is performed under the conditions of a steady flow, while the measurement is undertaken under unsteady (pulsating) flow conditions. As a result, transient values of the mass flow rate may be distinctly higher than the mean value – see Section 5. During the tests, pulse amplitudes comparable to the mean value were often met.

[3] For the circular cross-section of the straight pipe, the flow can be considered to be axisymmetric.

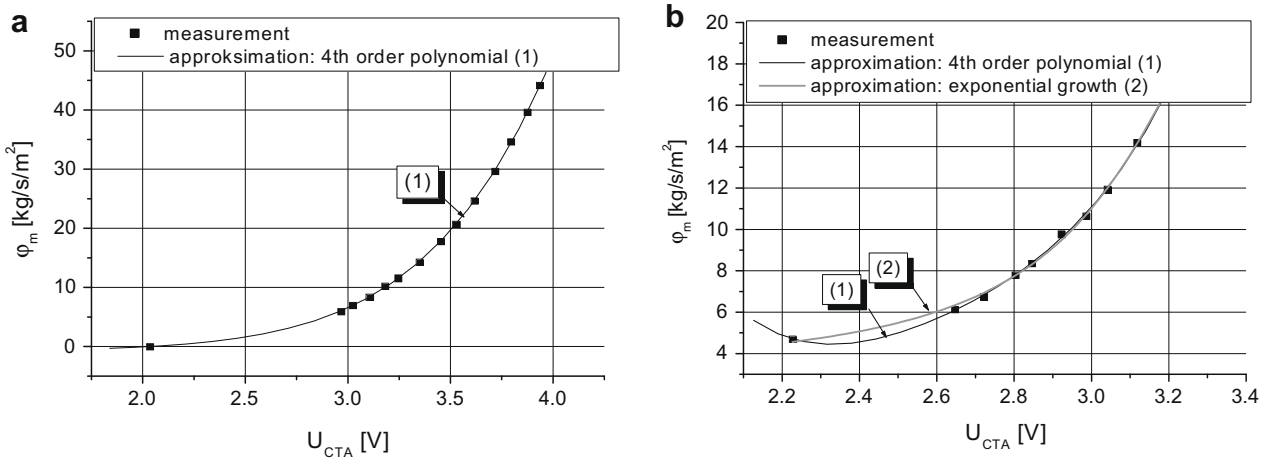

Fig. 2. Example calibration characteristics obtained for the hot-wire anemometers employed in the tests.

$$\dot{m}_{ref} = k_A \sqrt{\frac{p_A \Delta p_A}{T_A}} \tag{8}$$

where (see also Fig. 1a): k_A is the flow coefficient (defined by the manufacturer); p_A, the static pressure measured upstream of the probe; Δp_A, the Annubar differential pressure; and T_A is the static temperature upstream of the probe.

The flow coefficient k_A is considered to be independent of the flow velocity, as the special diamond-like shape of the Annubar sensor establishes a fixed separation point in a wide range of Reynolds numbers. A detailed analysis of uncertainties for specific mass flow rate measurements by means of the Annubar probe was presented in Olczyk (2008b). The calculations have shown that in the whole tested range, a relative uncertainty of the specific mass flow rate does not exceed 1%.

During the calibration and the measurements, both thin-wire probes (CTA and CCT) were mounted near the pipe axis to avoid an influence of the phenomena related to the presence of the boundary layer (Olczyk, 2008a).

The calibration was carried out in a range of mass flow rates supposed to be achieved during the measurements.

4. Measurement under the conditions of a pulsating flow

The concept of measurement was based on the assumption that when calibrated in the way described above, the hot-wire probe would measure the specific mass flow rate in one single point of the pipe cross-section,[4] but the voltage signal recorded in this way would correspond to the mean specific mass flow rate in the examined control section.

This approach allows us to consider the flow to be unsteady, but averaged spatially in the pipe cross-section. It also allows us to avoid the flow field survey and to use one single quantity representing the flow in the whole control section. It is also convenient from a practical point of view, because such a simplification permits us to use a 1-D description of the unsteady flow (Kazimierski et al., 1999) by means of parameters representing each section of the pipe in every moment of the analysis.

During the measurement procedure, signals from both CTAs (sections (0) and (3) see Fig. 1a) were recorded by means of a computer with a fast acquisition card (Keithley DAS 1801ST). The obtained sampling frequency was 10 kHz per channel. Then, voltage signals were converted into specific mass flow rates through the use of calibration characteristics and next approximated by a Fourier series. It was found that the first three harmonics were sufficient for a correct approximation of the signal (Olczyk, 2008a). Higher harmonics were considered to be noise (their amplitudes were less than 5% of the constant term).

Fig. 3 presents an example of measured specific mass flow rate plots in control sections (0) and (3) (Fig. 3a) together with their approximation by means of the first three harmonics (Fig. 3b).

The signals presented indicate a possibility of determining transient mass flow rate variations, representative of the whole control section on the basis of the point measurement only.

The basic criterion which should be satisfied in this case is such that the mean mass flow rates in the tested control sections are equal. The case presented shows a good coincidence of the constant terms $\bar{\varphi}_m = \varphi_{m\,ave}$[5] in the inlet and outlet sections (their difference is approximately 4%).

The situation described above appears in a wide range of tested frequencies, however for some of them, the recorded $\varphi_{m(t)}$ signals look surprising. Fig. 4a shows signals recorded for the short pipe in the system with a large volume tank at the frequency of 130 Hz. A huge disproportion of amplitudes at the pipe inlet and outlet is especially worth noting, as well as a quite different level of constant terms for these two sections. Also, the shape of the $\varphi_{m3(t)}$ signal is surprising as additional local maxima appear. What is important, there are no equivalent additional maxima in the recorded signals neither of pressure nor temperature (Olczyk, 2007). It should be also noted that the transition between the phases corresponding to global and local maxima (near zero) takes place without satisfying the condition of continuity of the first derivative.

The presented features of the recorded signal $\varphi_{m3(t)}$ indicate that, in fact, in some parts of the pulsation period, an inversion of the flow direction takes place. This is the phase of the reverse flow characterized by negative velocities (see Fig. 4b). As the CTA output signal depends on the quantity of heat exchanged between the wire and the flowing gas, the probe does not recognize the flow direction. An increase in the flow velocity is manifested by a more intensive heat exchange at the wire surface, which makes the CTA output signal higher, but the distinction of the flow direction is impossible. To reconstruct the true signal, a procedure of re-conversion (de-rectification) was applied in respective parts of the

[4] In practice the probe location corresponded to the position of the wire near to the pipe axis.

[5] The constant term corresponds to the averaged value in the time interval corresponding to a multiple of the pulsation period.

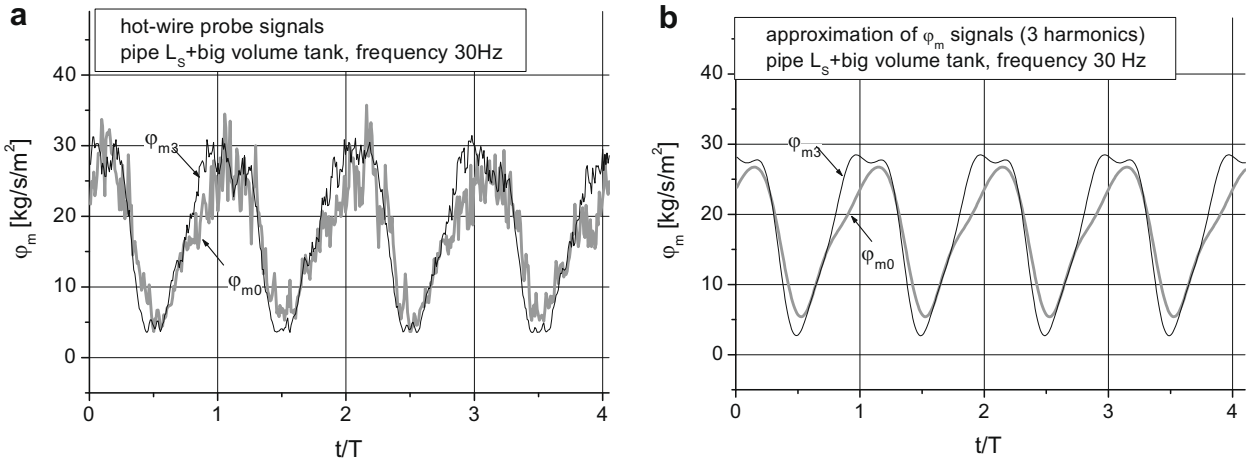

Fig. 3. Hot-wire probe signals φ_{m0} and φ_{m3} recorded in both the control sections (a) and their approximation by means of a Fourier series (b). Measurements for the short pipe (L_S) with a tank. Pulse frequency 30 Hz.

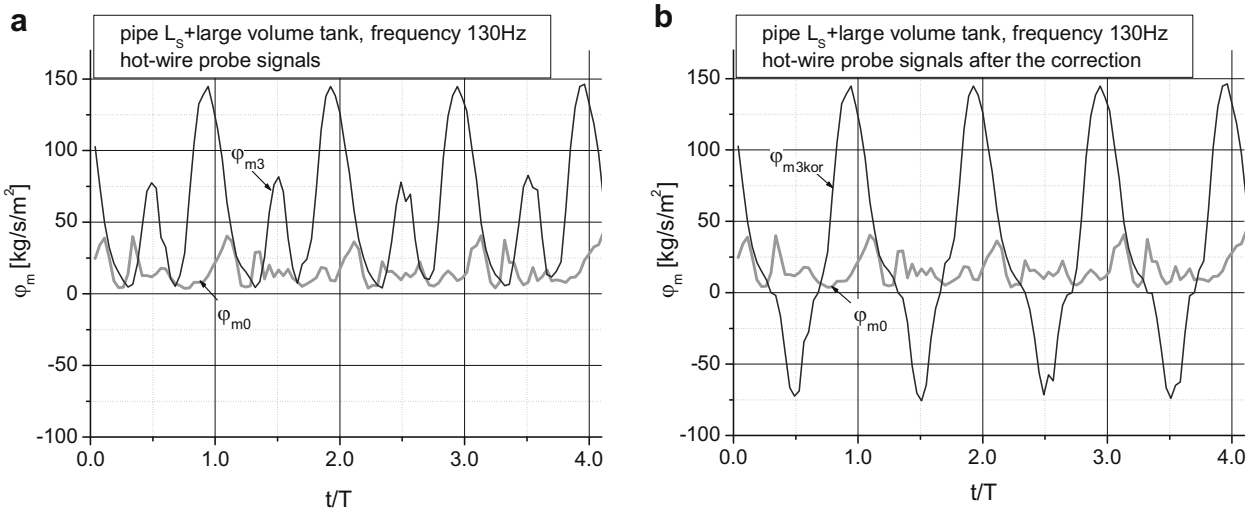

Fig. 4. Signals of φ_m recorded by hot-wire probes at the pulse frequency of 130 Hz (a) and the corresponding signals after the correction (b) that accounts for the reverse flow of gas. Results for the short pipe (L_S) with a large volume tank.

pulsation period. The effect of such a procedure is presented in Fig. 4b. As a result, the constant terms of the velocity signals for the inlet and outlet sections $\varphi_{m1\,ave}$ and $\varphi_{m3\,ave}$ approach one another.

The presence of the reverse flow was confirmed by numerical calculations conducted by means of the "x–t" model of a pulsating flow described in Kazimierski et al. (1999) and Olczyk and Sobczak, (2008). An example is shown in Fig. 5, where calculated and measured signals are compared, and a result of correction of the rectified signal is presented as well.

Fig. 6 shows intensification and retreat of the reverse flow in the neighborhood of the resonance frequency, which was determined to be equal to 140 Hz for the short pipe L_S (Olczyk, in press).

A question arises whether the determined temporal variations of the specific mass flow rate are representative as spatially averaged transient parameters describing the flow in the control section under analysis. In order to check this, the flow correction coefficient k_m was used (Olczyk and Hammoud, 1993):

$$k_{\dot{m}} = \frac{\bar{\dot{m}}}{\dot{m}_{ref}} \tag{9}$$

where:

$$\bar{\dot{m}} = \frac{S_p}{jT}\int_0^{jT} \varphi_{m_{(t)}}\,dt \tag{10}$$

where: T is the pulsation period and j is the number of periods used for analysis.

When $k_m = 1$ is obtained, it corresponds to a perfect coincidence of the averaged mass flow rate $\bar{\dot{m}} = \dot{m}_{ave}$ with the reference value $\dot{m}_{ref}$ measured by the Annubar probe.

Fig. 7a presents plots of the averaged mass flow rates $\dot{m}_{0\,ave}$ and $\dot{m}_{3\,ave}$ calculated from the recorded signals of $\varphi_{m0}(t)$ and $\varphi_{m3}(t)$ for the pipe L_S open at the end. Those plots were compared to the reference mass flow rate $\dot{m}_{ref}$. Three important observations can be made:

(i) as pressure in the air supply network is not fully stabilized, the reference mass flow rate varies slightly;
(ii) away from the resonance (in the range of low frequencies), both averaged mass flow rates are acceptably consistent with the reference value (see also plots of k_{m0} and k_{m3} – Fig. 7b);

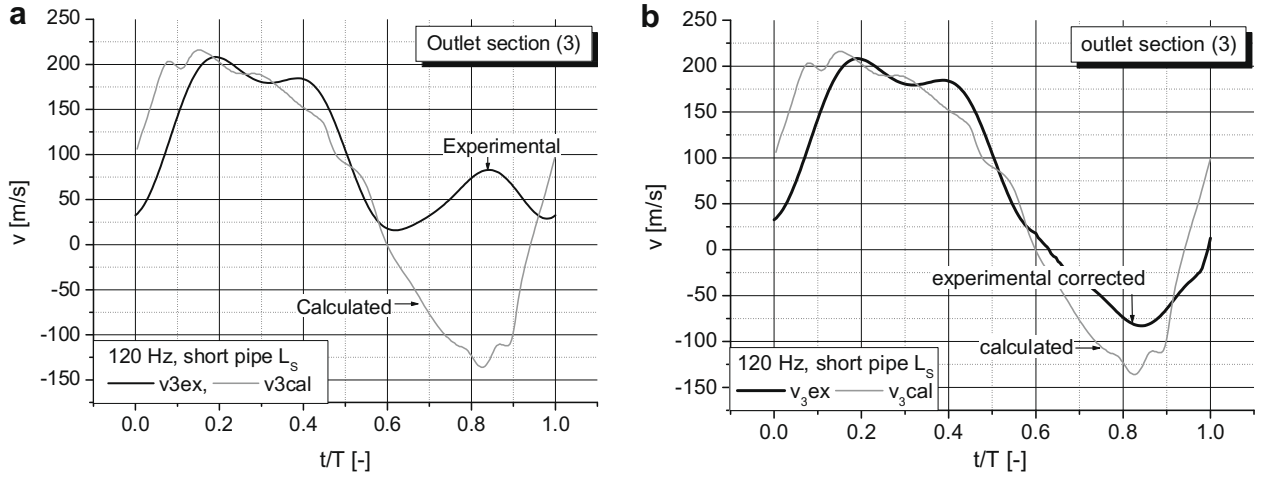

Fig. 5. Velocity signals at the pipe outlet section (3): v_{3cal} – calculated by means of the x–t model and v_{3ex} – experimental measured (a) and corrected (de-rectified – b). Results for the system with big volume tank at the pipe outlet and pulse frequency 120 Hz.

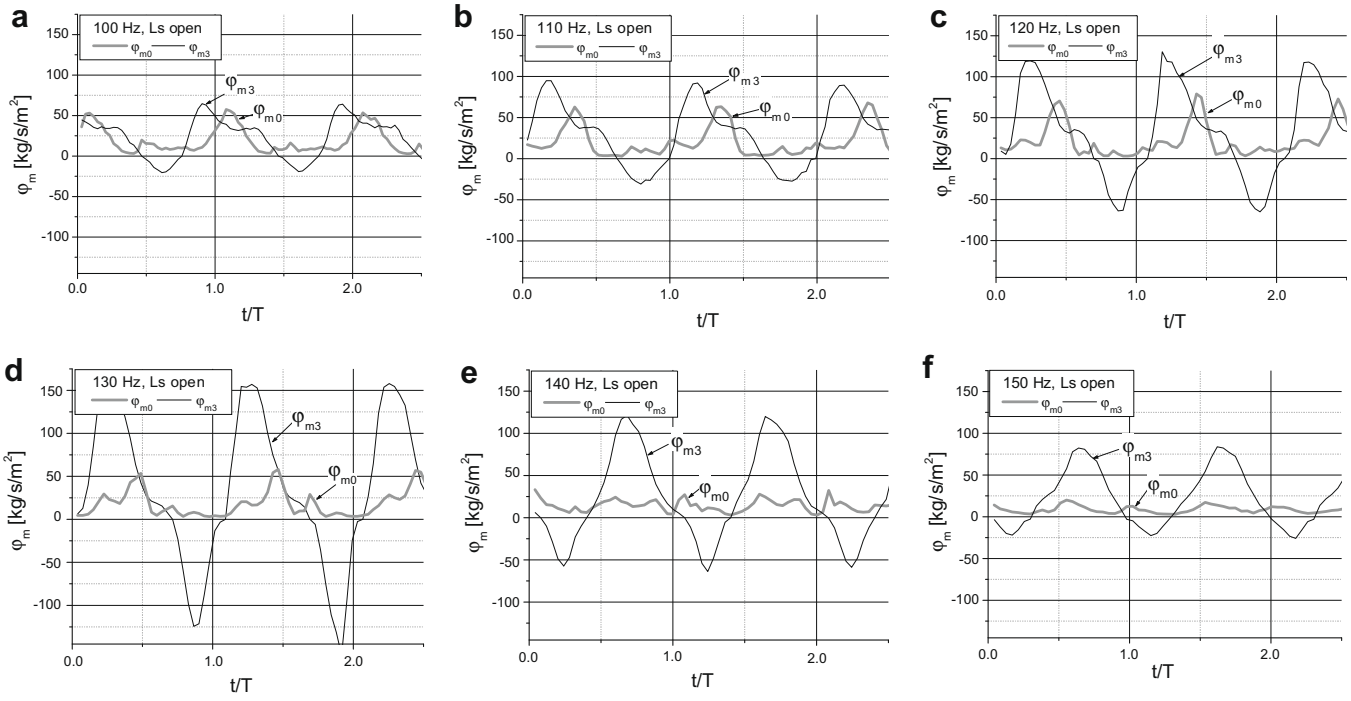

Fig. 6. Intensification and retreat of a reverse flow in the pipe open at the end in the neighborhood of the resonance frequency (130 Hz).

(iii) approaching the resonance (140 Hz), the two examined mass flow rates are no longer consistent with the reference value. In the direct resonance proximity, the mass flow rate at the outlet section is 75% higher than the reference. On the other hand, the inlet mass flow rate decreases rapidly having surpassed the resonance frequency.

After changing the pipe length, the resonance frequency is displaced. For the long pipe (L_L = 1.246 m), the resonance frequency is placed in the neighborhood of 60 Hz. Fig. 8a and b shows that phenomena observed for the long pipe are analogous to those for the short one. A divergence of the analyzed mass flow rates (up to 40%) for the resonance frequency and a rapid decrease of the mass flow rate at the inlet section are qualitatively equal.

If the averaged $\dot{m}_{ave}$ and reference $\dot{m}_{ref}$ specific mass flow rates are divergent, the correction of the recorded $\varphi_m(t)$ signal can be done by dividing it by the determined coefficient k_m in order to ensure the coincidence of mean values of φ_m in the control sections under investigation.

This correction is necessary for frequencies near the resonance, where an intensive reverse flow occurs and the amplitude of pulsations attains considerable values. During the calibration, which is conducted under the conditions of a steady flow, a volumetric compressor supplying the test rig permits to generate the maximum permanent mass flow rate $\dot{m}_{\max} = 0.1$ kg/s approximately, which corresponds to the specific mass flow rate of $\varphi_{\max}$ = 55 kg/sm^2 (see Fig. 2a). Thus, the obtained static characteristics, extrapolated for mass flow rates exceeding even three times the maximum value achieved during calibration, are no more adequate in the range of high flows (see the maximum values of $\varphi_{m3(t)}$ – Figs. 4b and 6d). That is why, in the neighbourhood of the resonance, the proposed procedure of correction seems to be a reasonable ap-

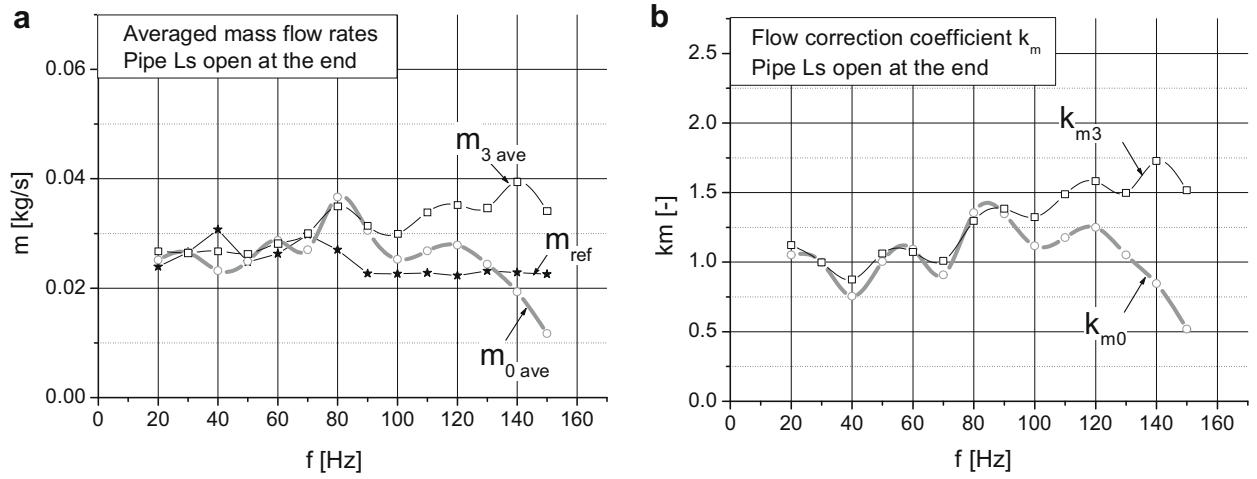

Fig. 7. Comparison of the averaged mass flow rates in sections (0) and (3) to the reference mass flow rate $\dot{m}_{ref}$ (a) and the $k_{\dot{m}}$ coefficient plots for these sections (b). Results for the pipe L_S open at the end.

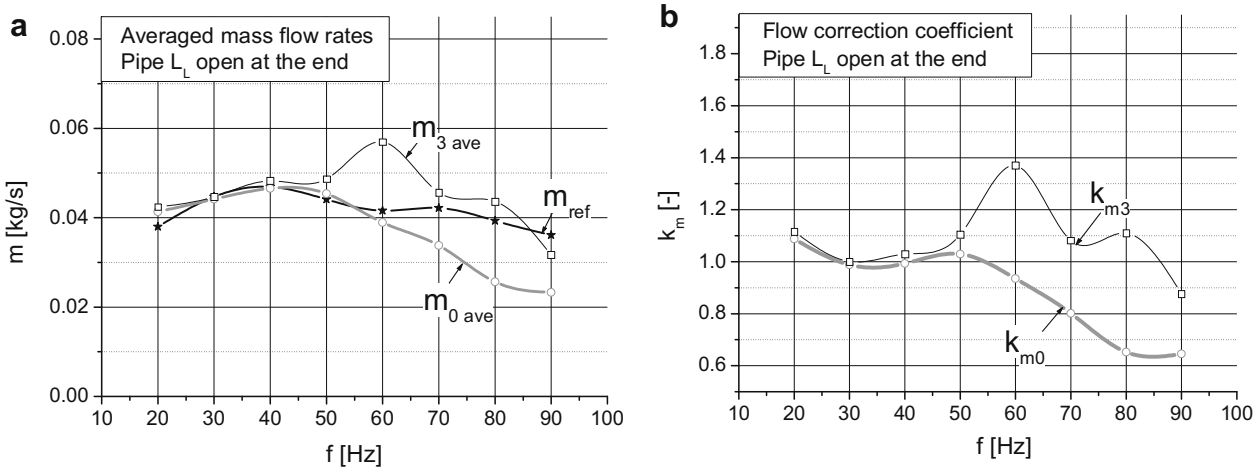

Fig. 8. Comparison of the averaged mass flow rates in sections (0) and (3) to the reference mass flow rate $\dot{m}_{ref}$ (a) and the $k_{\dot{m}}$ coefficient plots for these sections (b). Results for the pipe L_L open at the end.

proach, permitting for a correct description of the dynamic phenomena existing in this field.

5. Flow field investigation

In order to explain the observed phenomena, a flow field survey was carried out for steady (corresponding to the calibration conditions) and unsteady (corresponding to the measurement conditions) flows. Distributions of the specific mass flow rate were obtained by displacing both anemometric probes radially from the pipe axis ($r = 0$) towards the pipe wall ($r = 21$) with a step of 2 mm (1 mm in the direct wall proximity).

Some selected results for the short pipe open at the end and two different frequencies: 60 and 130 Hz are presented in Fig. 9a and b. For clarity, only selected characteristic curves are presented. The extreme curves, limiting the range of the survey, are $\varphi_{m\ (r=0)}$ and $\varphi_{m\ (r=20)}$. At the pipe wall ($r = 21$), the condition $\varphi_{m\ (r=21)} = 0$ must be satisfied. In order to compare successive plots recorded independently, in different time moments, the peak generator curve was applied. It shows a fully open position of the pulse generator. The distance between two successive peaks corresponds to two pulsation periods (the pulsation is generated twice per one revolution of the generator rotor).

The signals of $\varphi_{m(t)}$ recorded at successive radii for the frequency of 60 Hz show that variations of the specific mass flow rate are independent of the probe position in a relatively wide area around the pipe axis (Fig. 9a and b), plots from $r = 0$ to $r = 16$).

This area – by analogy to the steady flow – can be referred to as the flow core. It can be also observed in Fig. 10a where a relation of the averaged in time φ_{mave} versus the radial probe position is presented. Beyond the flow core, the pulsation amplitude decreases and the flow deceleration (a decrease in the mean value φ_{mave}) takes place. There is no important change in the pulsation shape (Fig. 9a and b) – the form of signals recorded at different radii is similar as far as their shape or phase shift is concerned. This observation is extremely important, because in the case of 1-D modeling, relationships between the velocity in the pipe axis and the shear stress at the pipe wall are necessary. Usually this relationship is assumed or calculated as shown in Kazimierski and Horodko (1990), Kazimierski et al. (1999) without experimental verification.

The plots of $\varphi_{m(t)}$ recorded for the resonance frequency 130 Hz are presented in Fig. 9c and d. Generally, the flow behavior is similar to that for the frequency of 60 Hz, however two important features are worth noting:

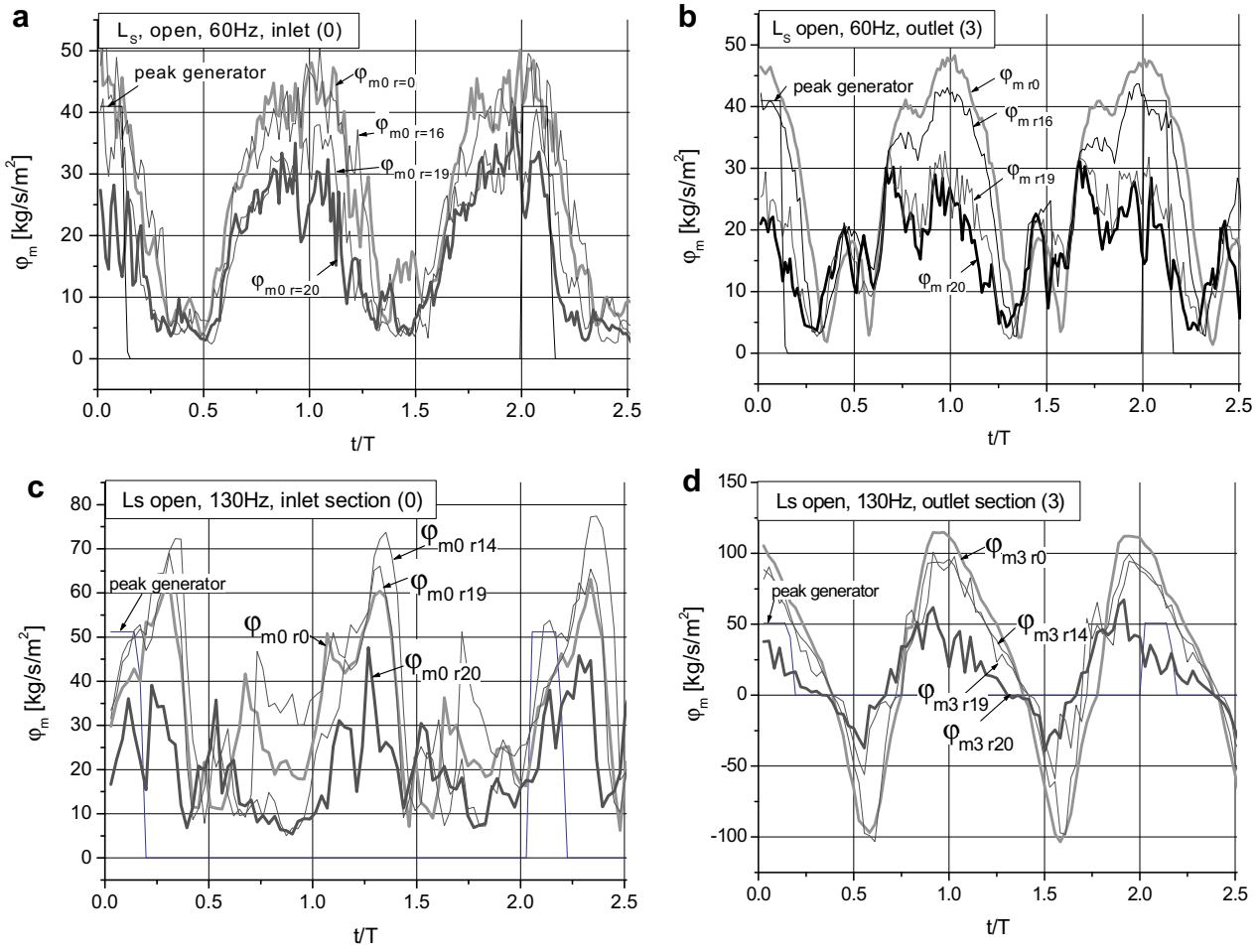

Fig. 9. Signals of the specific mass flow rate $\varphi_{m(t)}$ at the inlet (a, c) and outlet (b, d) sections of the pipe for different probe positions. Results for the pulse frequency 60 Hz (a, b) and 130 Hz (c, d). Measurements for the pipe L_S open at the end.

(i) at the pipe outlet (Fig. 9d), the most intensive reverse flow takes place. Its presence can be seen all over the control section, even in the direct proximity of the pipe wall (see the plot $\varphi_{m3\ (r=20)}$);

(ii) at the pipe inlet (Fig. 9c), the amplitude of $\varphi_{m(t)}$ in the pipe axis ($r = 0$) is no longer maximum (as it was for lower frequencies). It can be seen that this amplitude increase attains the maximum value for ($r = 14$) and then starts to decrease, however this decrease is sharp only in the direct proximity of the wall. It is hard to find a definite explanation for such a behaviour. Probably the obtained velocity distribution is a result of specific features of the pulse generator applied.

Fig. 10a and b shows distributions of the mean specific mass flow rate in the inlet and outlet sections of the pipe for the tested frequencies compared to the profile obtained for steady flow conditions. The following observations can be made:

(i) the $\varphi_{m\,ave(t)}$ profile is much more uniform under the conditions of a pulsating flow (compare the plots of $\varphi_{m\,ave\_0\,Hz}$ and $\varphi_{m\,ave\_60\,Hz}$ for both inlet and outlet sections). It is due to a more intensive momentum exchange between flow regions located at different radii. Under the conditions of a steady flow, even though the mean Reynolds number calculated for the pipe axis is $Re_{(r=0)} = 0.61 \times 10^5$, which clearly indicates the presence of a turbulent flow, the distribution of the specific mass flow rate shows that the flow deceleration starts relatively close to the pipe axis.

The Reynolds number :

$$Re_{(r=0)} = \frac{\rho v d}{\mu} = \frac{\varphi_m d}{\mu} \tag{11}$$

was calculated for the following parameters: specific mass flow rate $\varphi_m = 25\ \mathrm{kg^1 s^{-1} m^{-2}}$ - compare Fig. 10a and b; pipe diameter $d = 0.042$ m and dynamic viscosity $\mu = 17 \times 10^{-6}\ \mathrm{kg^1\ m^{-1}\ s^{-1}}$ (Olczyk, 2008a);

(ii) the $\varphi_{m\,ave(t)}$ profile obtained at the pipe inlet for the resonance frequency (130 Hz) differs significantly from the two others. Like in the case of amplitudes (Fig. 9c) the mean value of $\varphi_{m\,ave}$ reaches its maximum off the pipe axis. In consequence, the signal measured by the wire located at ($r = 0$) is not fully representative of the mean mass flow rate in the control section of the pipe. As the specific mass flow rate profile changes, the coefficient k_{m0} (Fig. 8b) starts to decrease;

(iii) a slight increase of $\varphi_{mr=0)}$ at the pipe axis can be observed when the pulse frequency is increased. In order to compare successive plots without considering this relationship, the relative mass flow rate was defined as:

$$\varphi_{m\,rel} = \frac{\varphi_{m(r)}}{\varphi_{m(r=0)}} \tag{12}$$

The plots of $\varphi_{m\,rel}$ are presented in Fig. 10c and d.

The distributions of the specific mass flow rate obtained were also compared to the Prandtl distribution, usually employed for a

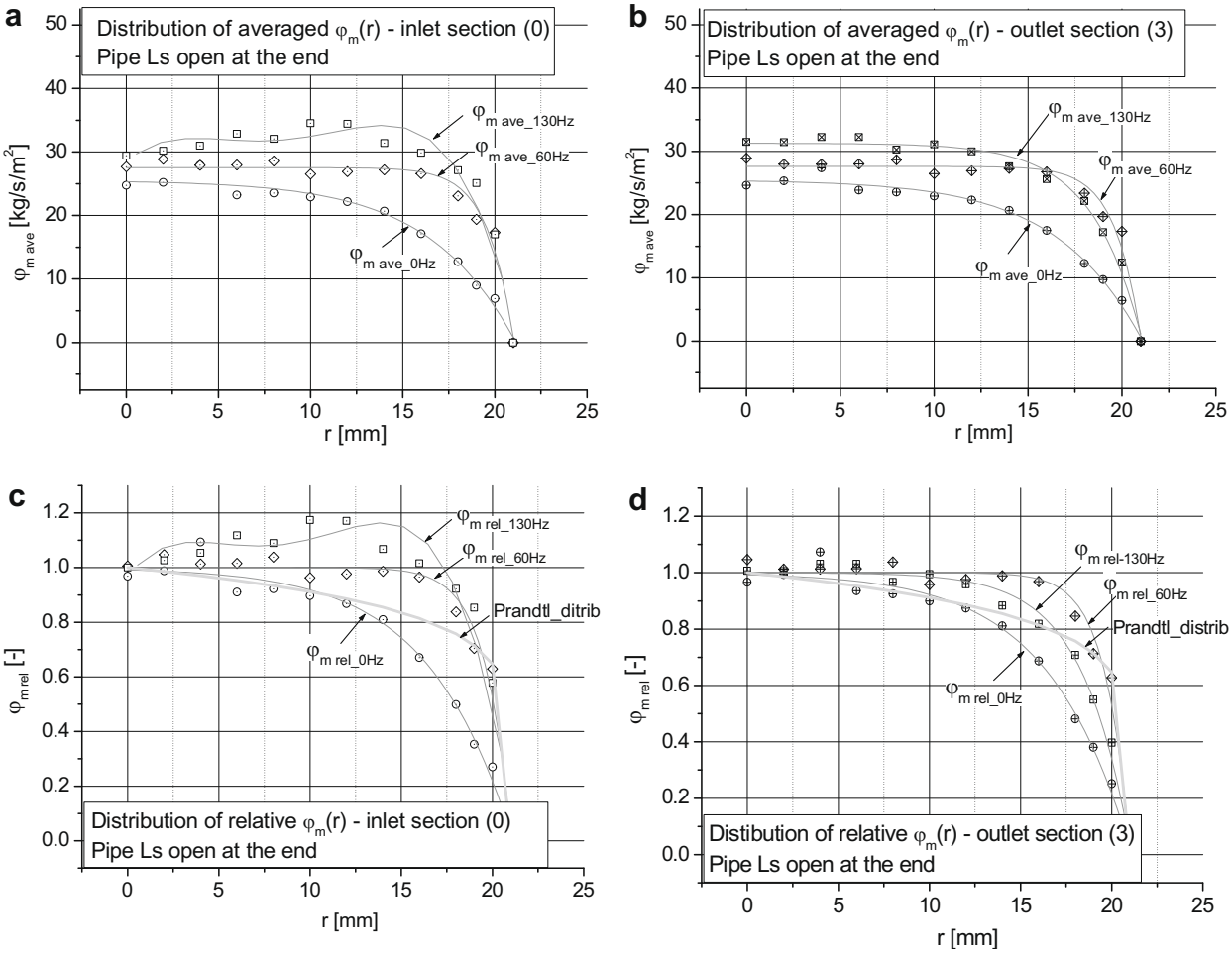

Fig. 10. Distributions of the absolute (a, b) and relative (c, d) mean specific mass flow at the tested control sections. Measurements for the short pipe (L_S) open at the end for a steady flow (0 Hz) and a pulsating flow (the frequency of 60 and 130 Hz).

description of the flow fields in circular section ducts (Fig. 10c and d) and described by the equation:

$$\varphi_{m_{(r)}} = \varphi_{m(r=0)}\left(1 - \frac{r}{R}\right)^{\frac{1}{n}} \tag{13}$$

where: R is the pipe radius; $1/n$, the exponent determined experimentally (depending on the Reynolds number and pipe wall roughness) – for the presented case, it was assumed that $n = 7$.

In the proximity of the pipe axis (up to $r = 12$), the Prandtl distribution corresponds quite well to the profile determined experimentally for a steady flow. Towards the pipe wall, these two profiles become divergent – the specific mass flow rate decrease is much faster for the experimentally determined curve. On the contrary, profiles determined for the unsteady flow stay flat in a larger zone (with an exception of the inlet profile for the resonance frequency), as discussed above.

Generally, the Prandtl distribution is not adequate for the determined profiles, and an approximation by means of the Boltzmann equation is proposed:

$$\varphi_{m(r)} = \varphi_{m(r=0)} + \frac{\varphi_I - \varphi_{m(r=0)}}{1 + e^{(r-r_I)/r_{II}}} \tag{14}$$

where: $\varphi_{m(r=0)}$ is the mean value of the specific mass flow rate in the pipe axis (for $r = 0$); and φ_I, r_I, r_{II} is the equation coefficients.

The results of such an approximation are shown in Fig. 10. Only the $\varphi_{m\,rel}$ curve for 130 Hz (Fig. 10a and c) was approximated by means of the 4th order polynomial.

6. Conclusions

The presented method of measurement of the transient mass flow rate in ducts supplied with a pulsating flow allows us to obtain quite precise information concerning the character of these variations, including the case of a reverse flow, which makes an interpretation of the recorded signals difficult.

The point measurement of the specific mass flow rate conducted by means of a hot-wire probe can be considered to be representative for the whole section, provided that the correct assignment of the voltage signal to the appropriate specific mass flow rate is achieved. An ideal case is when the velocity profile is uniform. This condition is nearly satisfied in the case of the pulsating flow, as its character is distinctly turbulent, with an exception of the narrow region of the boundary layer in the direct proximity of the pipe wall. Under these conditions, the velocity profiles obtained for both inlet and outlet sections are very similar, which ensures balancing of the mean mass flow rate in these sections.

In the case of the resonance existing in the pipe for characteristic frequencies depending on the pipe length, an intensive reverse flow occurs and the correction procedure, which takes into account the effect of an inversion of the velocity direction, should be applied. The resonance range is characterized by high pulse amplitudes, exceeding several times the mean value of the recorded signals. Under these conditions, maximum transient values of the specific mass flow rate go far beyond the range of calibration characteristics drawn for steady flow conditions. This is why, an addi-

tional signal correction is necessary by means of the flow correction coefficient k_m determined experimentally with a standard flowmeter and recording the reference flow upstream of the pulse generator, under the conditions of a steady flow.

The proposed method is especially useful in cases applying 1-D models of pulsating flows in tubes, as it allows us to handle flow parameters attributable to the pipe axis, but representative of the whole control section.

The flow field survey shows that the character of mean specific mass flow rate profiles can vary depending on the flow character (steady, unsteady) and the pulse frequency.

References

Al-Garni, A.M., 2007. Low speed calibration of hot-wire anemometers. Flow Measur. Inst. 18, 95–98.

Bremhorst, K., Graham, L.J.W., 1990. A fully compensated hot/cold wire anemometer system for unsteady flow velocity and temperature measurements. Measur. Sci. Technol. 1, 425–430.

Breuer, M., Schernus, C., Bowing, R., Kuphal, A., Lieske, S., 2000. Experimental approach to optimize catalyst flow uniformity. SAE Paper 2000-01-0865.

Bruun, H.H., 1999. Hot Wire Anemometry – Principles and Signal Analysis. Oxford University Press.

Bruun, H.H., Farrar, B., Watson, I., 1989. A swinging arm calibration method for low-velocity hot-wire probe calibration. Exp. Fluids 7, 400–404.

Chalet, D., Chesse, P., Tauzia, X., Hetet, J.-F., 2006. Comparison of different methods for the determination of pressure wave in the inlet and exhaust systems of internal combustion engine. SAE Paper 2006-01-1542.

Cimbala, J.M., Park, J.W., 1990. A direct hot-wire calibration technique to account for ambient temperature drift in incompressible flow. Exp. Fluids 8, 299–300.

Dieterich Standard, 1995. Annubar flow measurement system. Product Catalog. Dieterich Standard.

Elsner, J.W., Gundlach, W.R., 1973. Some remarks on the thermal equilibrium equation of hot-wire probes. DISA Information No. 14.

Endevco, 2003. Piezoresistive pressure transducers. Instruction Manual, Endevco Corp.

Handford, P.M., Bradshaw, P., 1989. The pulsed-wire anemometer. Exp. Fluids 7, 125–132.

Lu, Jau-Huai, Sheu, Yoeu-Wei, Liu, Der Jen, Hsiao, Chih-Wei, 1998. Cycle-resolved flow measurements in the exhaust pipe of single-cylinder, two-stroke engines. SAE Paper 980759.

Kazimierski, Z., Horodko, L., 1990. Total pressure averaging by small-diameter tubes in flows. AIAA Journal 28, 140–145.

Kazimierski, Z., Rabiega, M., Sobczak, K., 1999. One-dimensional model of pulsating viscous flow in tubes. In: International Conference on SYMKOM'99, Turbomachinery, vol. 115, pp. 191–200.

King, L.V., 1914. On the convection of heat from small cylinders in a stream of fluid. Philos. Trans. – Royal Soc. Lond. Ser. A 214.

Kirkpatrick, S.J., Blair, G.P., Fleck, R., McMullan, R.K., 1994. Experimental evaluation of 1-D computer codes for the simulation of unsteady gas flow through engines – a first phase. SAE Paper 1994 941685.

Ligęza, P., 2008. Optimisation of single sensor two-state hot-wire anemometer transmission bandwidth. Sensors 8, 6747–6760.

Olczyk, A., Hammoud, A.A., 1993. Les problèmes des mesures de débit instantané à l'aide d'une sonde a fil chaud. Turbomachinery 686, 187–209.

Olczyk, A., 2007. Influence of unsteady flow phenomena in the turbine inlet pipe on the turbocharger performance. Final Report of the Polish State Committee for Scientific Research Project No. 4T12C03828, Archives of the Institute of Turbomachinery, Technical University of Lodz, No. 1569 (in Polish).

Olczyk, A., 2008a. Problems of unsteady temperature measurements in a pulsating flow of gas. Measur. Sci. Technol., 19 (Paper 055402).

Olczyk, A., Sobczak, K., 2008 Contribution to one-dimensional model of a pulsating flow of gas in application to turbocharger inlet pipes. In: International Conference on SYMKOM'2008, Turbomachinery, vol. 133. pp. 263–270.

Olczyk, A., 2008b. Uncertainty analysis in case of the mass flow rate measurement by means of multihole impact probes. Turbomachinery 134, 43–58.

Olczyk, A., in press. Identification of dynamic phenomena in pipes supplied with a pulsating flow of gas. J. Mech. Eng. Sci.

Omega Inc., 2000. The Temperature Handbook. 21st ed. Omega Engineering Inc.

Sakao, F., 1973. Constant temperature hot wires for determining velocity fluctuations in an air flow accompanied by temperature fluctuations. J. Phys. E: Sci. Instrum. 6, 913–916.

Savostenko, P.I., Serbin, S.P., 1988. Hot-wire anemometer invariant to temperature of the medium. Meas. Technol. 31 (12), 1174–1178.

Sokolov, M., Ginat, Z., 1992. The ladder probe: reverse flow measurement with a hot-wire rake. Exp. Fluids 12, 307–318.

Shibl, A., 1987. Empirical expression for hot-wire with corrections for temperature drift. Wärme und Stoffübertragung 21, 329–332.

Thompson, B.E., Whitelaw, J.H., 1984. Flying hot-wire anemometry. Exp. Fluids 2, 47–55.

TSI Inc. Advantage to the look-up table approach of voltage-velocity conversion in thermal anemometry. Technical Note. TSI website: <http://www.tsi.com>.

Witze, P.O., 1980. A critical comparison of hot-wire anemometry and laser Doppler velocimetry for I.C. engine applications. SAE Paper 800132.